The University of Osaka
Institutional Knowledge Archive

The University of Osaka Institutional Knowledge Archive : OUKA

https://ir.library.osaka-u.ac.jp/

The University of Osaka

Generation and Reduction of Residual Stress in Ceramic/Metal Joints[†]

You Chul KIM*, Tetsuya YAMAMOTO** and Tom H. NORTH***

Abstract

Methods for crack prevention during ceramic/metal joining are suggested based on the results of a detailed mechanical analysis. The characteristics of the distribution of residual stress produced during solid-state bonding of Si_3N_4 to steel is elucidated based on the results of a thermal elastic-plastic analysis. The principal factor which promotes crack formation is the bending moment which acts on the ceramic substrate; this is caused by the difference in thermal expansivities of the metal and ceramic substrates. It is suggested that this bending moment should be minimised in order to prevent crack formation in the ceramic substrate. The validity of this approach has been confirmed based on detailed calculations. In addition, the effectiveness of laboratory test specimen designs for measuring the bonded strength of ceramic/metal joints are elucidated, and geometries which facilitate easy specimen manufacture produce lower bending moment and the maximum stress value perpendicular to bonded line than in actual fabricating situations.

KEY WORDS :(Residual deformation)(Residual stress)(Thermal elastic-plastic analysis)(FEM)(Modeling) (Dissimilar materials)(Solid state bonding)

1. Introduction

The service conditions to which components are subjected are becoming increasingly severe in industry and this has placed even greater demands on material requirements. Because of this, there is particular interest in the application of components which comprise structural ceramics and metals *working in combination*. Structural ceramics and metals can be used successfully together only if solutions are provided for a range materials science and mechanics problems[1-2]. In particular, satisfactory ceramic/metal joining depends on solving the mechanics problem associated with crack formation in the ceramic substrate. In this connection, the mechanical situation in dissimilar joints [3], and the diverse effects of material mechanical properties and dimensions on residual stress formation have already been examined using thermal elastic analysis [4].

This paper uses thermal elastic-plastic modeling to examine the residual stress generated in solid-state joints between Si_3N_4 and SM50 steel substrates. The factors which determine the magnitude and distribution of residual stress are elucidated and a methodology for crack prevention is developed and validated. The influence of insert layer yield stress and thickness, of joint configuration (geometry) on residual stress formation is examined in detail.

2. Residual Stress Generation in Solid-State Bonding

The finite element calculations consider the situation which occurs when Si_3N_4 ceramic is diffusion bonded to SM50 steel and elucidate the mechanism of residual stress generation in detail.

2.1 Modeling approach

Solid-state bonding involves heating the samples in a vacuum furnace and, when the bonding temperature is attained, the joint is produced by upsetting the two samples for a given holding time. Since the substrates can expand freely during the heating cycle no stress is generated during this period. Upsetting pressure is required to disrupt the oxide film on the substrate surfaces, to bring the specimens into intimate contact, and to speed up solute diffusion at the bonding temperature. The magnitude of the upset stress is extremely low, 20-30 MPa [5].

It is well-known that the critical temperature T_m below which the metal has measurable mechanical properties (yield stress etc.) is much less for the SM50 steel material than it is for the ceramic substrate. As a result, the steel may be considered to be fully plastic at the diffusion bonding temperature. With this in mind, the mechanical situation in diffusion bonding can be satisfactorily modelled by considering the cooling cycle only, and the temperature range from T_m (700 °C) to room temperature in particular. The finite element model applied in this study is illustrated in **Figure 1**; this joint configuration will be referred to as the *standard model* for the remainder of this paper. The mechanical
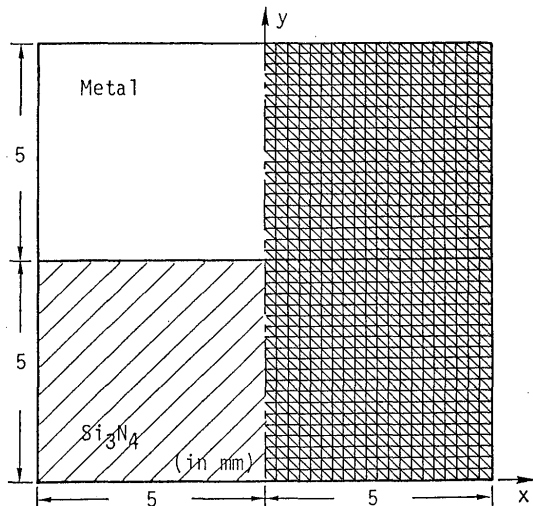
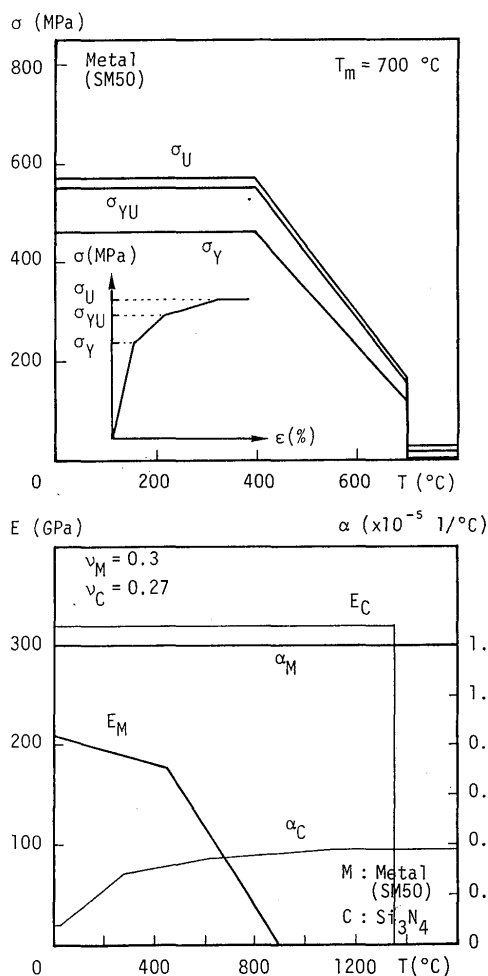Fig.1 Standard model employed in the finite element analysis and grid.

Fig.2 Temperature dependency of silicon nitride and SM50 steelmechanical properties.

property/temperature relations for SM50 steel and silicon nitride are presented in **Figure 2**. Si_3N_4 is considered fully elastic, the steel is elastic-plastic and the thermal elastic-plastic analysis is carried out as a plane stress problem using the finite element method.

2.2 Features of residual stress generation

Figure 3 shows the residual deformation produced when the dissimilar joint is cooled from 700 °C to room temperature. At the joint interface, it is found that the SM50 steel is prevented from shrinking freely. Due to the difference in the thermal expansivities of the ceramic and the steel, the deformation applied to the ceramic substrate may be equivalent to that when it is acted on by a counterclockwise bending moment.

Figure 4 shows the distribution of residual stress components (the σ_x component parallel to the bondline, the σ_y component perpendicular to the bondline and the shear component τ_{xy}) along the x- and the y-axis; the position, where the maximum value of each stress component occurs in the ceramic substrate, is also indicated.

The σ_x component within the ceramic is linearly distributed[6] and attains its maximum tensile value, $(\sigma_x)_{max}$, near the middle of the substrate base (at the co-ordinates x = 0.125 mm, y = 0.125 mm). This is indicated by the symbol ● in Figure 4(a). σ_x is compressive at the bondline and has a maximum value, $|\sigma_x|_{max}$, which occurs at symbol □ in Figure 4(a).

$$|\sigma_1|_{max} = 488.6 \text{ MPa}$$
$$\text{at } \begin{array}{l} x = 4.875 \\ y = 4.375 \end{array} \text{ (mm)}$$

$$|\sigma_2|_{max} = -775.1 \text{ MPa}$$
$$\text{at } \begin{array}{l} x = 0.375 \\ y = 4.875 \end{array} \text{ (mm)}$$
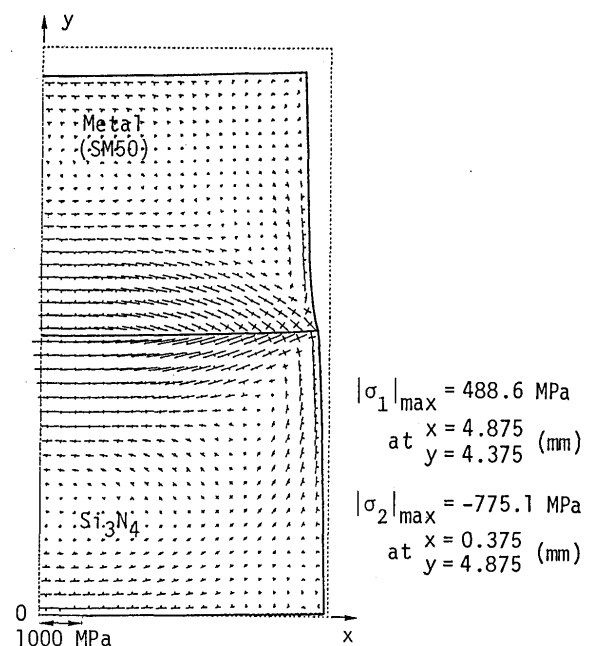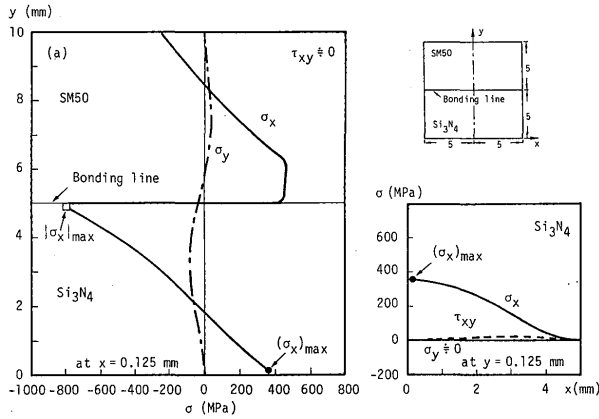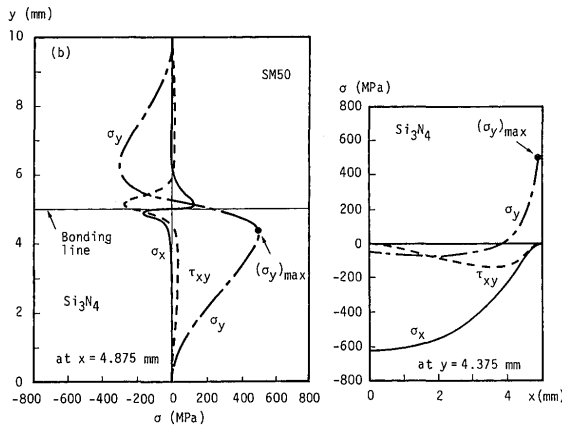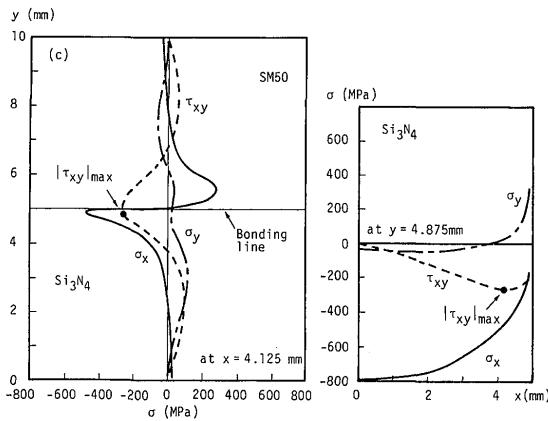
Fig.3 Deformation after dissimilar joining and vectors of principal stress, σ_1 and σ_2 (Standard model).

(a) Location where σ_x is maximum in Si₃N₄ and its magnitude.

(b) Location where σ_y is maximum in Si₃N₄ and its magnitude.

(c) Location where τ_{xy} is maximum in Si₃N₄ and its magnitude.

Fig.4 Residual stress distributions (Standard model).

The σ_y component attains its maximum value, ($\sigma_y)_{max}$, in ceramic material immediately below and perpendicular to the bondline, at the specimen periphery (at co-ordinates x = 4.875 mm, y = 4.375 mm in Figure 4(b)). It is suggested that ($\sigma_y)_{max}$ is closely associated with crack initiation at the periphery of the ceramic substrate (this idea will be discussed in detail later). **Figure 5** shows the relation between temperature and the transient tensile stress. ($\sigma_y)_{max}$ increases linearly in the temperature range 700 °C to 400 °C (see Figure 5 : the solid line) and then deviates from linearity at lower temperatures because the SM50 steel becomes plastic in this temperature regime (see Figure 2).

The maximum value of the shear component $|\tau_{xy}|_{max}$ (in Figure 4(c)) occurs near the sample periphery, immediately below the bondline (at the co-ordinates x = 4.125 mm, y = 4.875 mm). It follows that a joint between substrates which have widely differing mechanical properties produces a shear component which is largest adjacent to the bondline. Ignoring the shear stress component notation, the principal stress components, σ_1 and σ_2, can be obtained from the relation,

$$\begin{Bmatrix} \sigma_1 \\ \sigma_2 \end{Bmatrix} = \frac{1}{2}(\sigma_x + \sigma_y) \pm \frac{1}{2}\sqrt{(\sigma_x - \sigma_y)^2 + 4\tau_{xy}^2} \quad (1)$$

Figure 3 shows the vectors of principal stress components, σ_1 and σ_2, and Figure 6 shows the magnitudes of σ_1 and σ_2, at the location where σ_1 attains its maximum value, $|\sigma_1|_{max}$. The location of
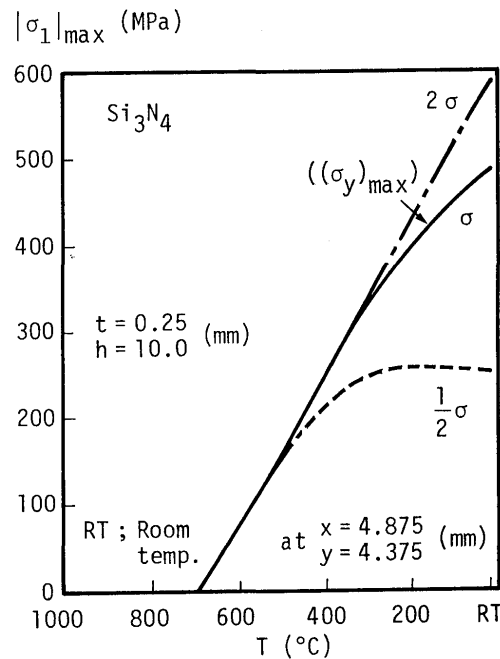

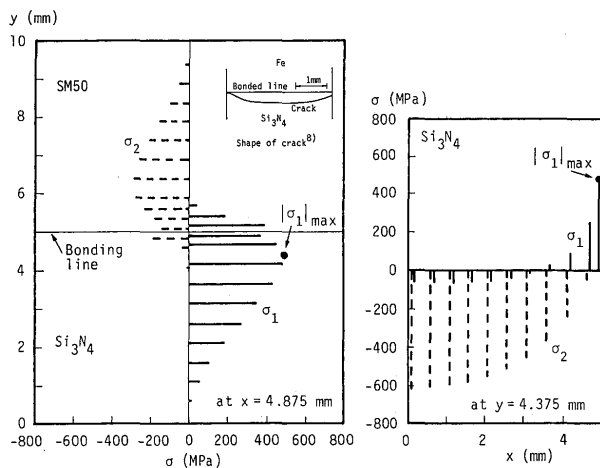Fig.5 Transient of maximum principal stress component, $|\sigma_1|_{max}$.

Fig.6 Magnitude of principal stress, σ_1 and σ_2, along the
x- and y-axes (Standard model).

$|\sigma_1|_{max}$ is coincident with that for the maximum tensile value of $(\sigma_y)_{max}$. σ_2 attains strongly compressive along the bondline. Based on Figures 3 and 6, the shape of a crack detected in a solid-state joint between silicon nitride and steel mirrors the vectors of principal stress[7]. Consequently, it is suggested that the maximum principal stress value ($|\sigma_1|_{max}$) is associated with crack initiation and that the direction of crack propagation depends on the σ_2.

As above mentioned, the distribution of σ_x (and σ_2) along the y-axis in the ceramic substrate (see Figure 4(a)), at the middle of the sample (x = 0), is compressive near the bondline and is tensile in the lower part. It follows that a large counterclockwise bending moment acts on the ceramic substrate. Therefore, if this bending moment can be reduced by some means, this will inhibit crack initiation since the $|\sigma_1|_{max}$ value produced during dissimilar joining will be decreased. This idea is developed in the next section.

3. Reducing Residual Stress: Consideration

This section investigates methods of reducing the $|\sigma_1|_{max}$ produced by the dissimilar joining operation. In the first instance, residual stress reduction caused by plastic flow in an insert layer material is considered. In the subsequent section, the effect of changing the joint configuration is discussed.

3.1 Reducing residual stress by plastic flow in the insert layer

It is well-known that placing insert layers between the ceramic and metal substrates promotes improved joint strength during dissimilar joining[8-9]. The main purpose of this section is to provide guidelines for selection of the insert layer material (based on the mechanical analysis).

3.1.1 Effect of interlayer strength

The thermal elastic-plastic analysis was carried out assuming that the magnitudes of σ_Y, σ_{YU} and σ_U (in Figure 2) are half, equal and double the value employed in the standard model. The insert layer thickness was t = 0.25 mm throughout. **Figure 7** confirms that decreasing the yield stress of the insert layer lowers the $|\sigma_1|_{max}$ value. Consequently, the use of a low yield stress ductile insert layer material will effectively reduce $|\sigma_1|_{max}$.

Figure 8 shows the residual deformation and the vectors of σ_1 and σ_2 when the insert layer yield stress is decreased by 50%.

3.1.2 Influence of insert layer thickness

The thermal elastic-plastic analysis was carried out assuming that the insert layer yield stress was half that in the standard model, and that the insert layer thickness was variable. **Figure 9** shows that the $|\sigma_1|_{max}$ and $|\sigma_2|_{max}$ values depend on insert layer thickness, and that $|\sigma_1|_{max}$ is lowest when the insert layer thickness is in the range, t = 0.1 mm to 0.2 mm.

Irrespective of the insert layer thickness, however, $|\sigma_1|_{max}$ occurs at the joint periphery, in ceramic substrate material adjacent to the bondline (at co-ordinates x = 4.875 mm, y = 4.375 mm). $|\sigma_2|_{max}$ is located at the middle, in ceramic substrate immediately below to the bondline (at co-ordinates x = 0.125 mm, y = 4.875 mm). Also, the directions of principal stress are not markedly different from those in the standard model. Consequently, the vectors of principal stress and the locations where they attain maximum values are not changed.

There is an optimum insert layer thickness and the insert layer should have low yield stress and high ductility.
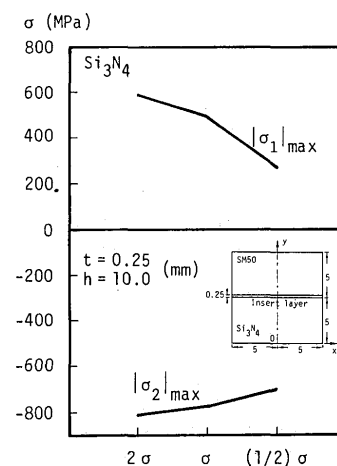

Fig.7 Effect of insert layer yield stress on the $|\sigma_1|_{max}$ value. The yield stress of the insert layer ranges from 50% to 200% of the initial value considered in Fig.2.
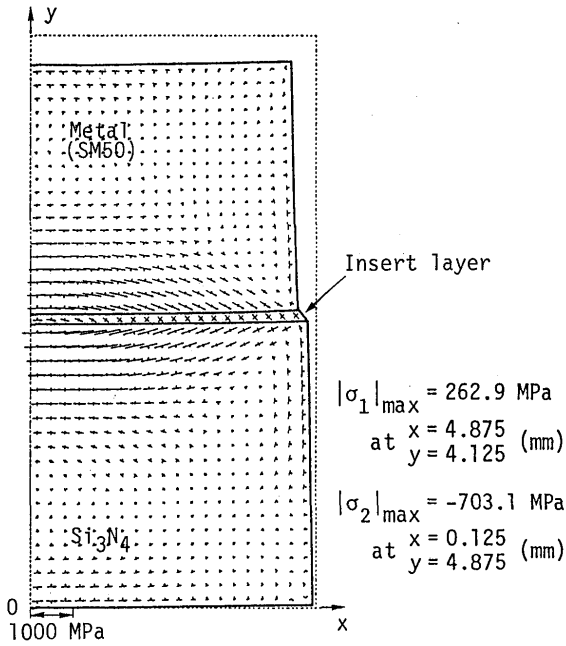
Fig.8 Deformation after dissimilar joining and vectors of principal stress, σ_1 and σ_2 (with insert layer).
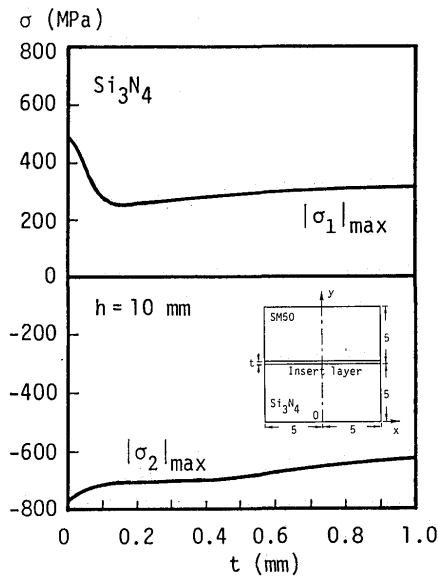

Fig.9 Effect of insert layer thickness on the maximum principal stress, $|\sigma_1|_{max}$ and $|\sigma_2|_{max}$.

However, it is important to point out that the final joint strength of dissimilar joints will not be detrimentally influenced by the yield stress of the insert layer employed.

3.2 Reducing residual stress by changing the joint configuration

This section investigates method of reducing the anticlockwise bending moment produced by the dissimilar joining operation. Particular emphasis is placed on examining the influence of different joint configurations on residual stress generation.

3.2.1 Use of sandwich assemblies

The joint configuration in **Figure 10(a)** shows the effect of sandwiching the SM50 steel substrate between two Si_3N_4 substrates. The thermal elastic-plastic analysis for this configuration produces a $|\sigma_1|_{max}$ value which is 70% of that produced in the standard model joint configuration.

If the joint configuration is arranged so the ceramic substrate is placed in the middle of the sandwich, the value of $|\sigma_1|_{max}$ is dramatically increased (it is 35% higher than that in the standard model). This occurs since an elastic material is placed at the center of the sandwich, its thickness is not great and consequently the contribution from the other bonded surface is also superimposed. This situation only occurs when the ceramic substrate is thin; when the ceramic thickness increases, the $|\sigma_1|_{max}$ value equals that in the standard model.

3.2.2 Varying the neutral axis of bending

Changing the neutral axis of bending will alter the anticlockwise bending moment produced by the joining operation. The $|\sigma_1|_{max}$ value is lowered to 85% of that in the standard model (in **Figure 10(b)**) and to 60% of that in the standard model (in **Figure 10(c)**). If the ceramic and steel substrates are reversed in Figure 10(b), however, the value of $|\sigma_1|_{max}$ value is 13% higher than that produced in the standard model joint configuration. This occurs since $|\sigma_1|_{max}$ is further from the bondline and consequently the anticlockwise bending moment is significantly increased.
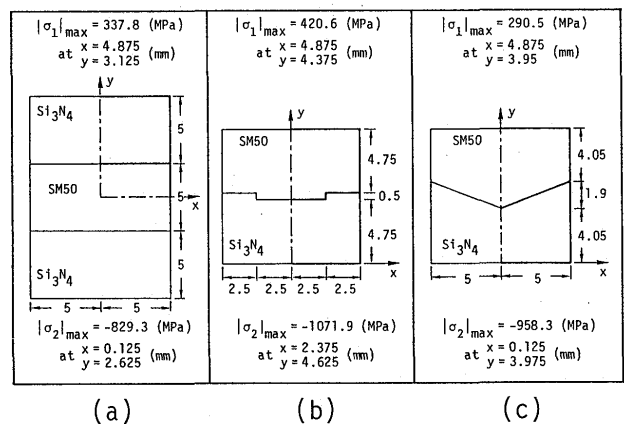

(a)   (b)   (c)

Fig.10 Effect of joint configuration (sandwiching the substrates, and varying the neutral axis) on the $|\sigma_1|_{max}$ value.

$|\sigma_1|_{max} = 381.4$ (MPa) at $\begin{array}{l} x = 5.125 \\ y = 4.875 \end{array}$ (mm)

$|\sigma_2|_{max} = -809.2$ (MPa) at $\begin{array}{l} x = 1.375 \\ y = 4.875 \end{array}$ (mm)

(a)

$|\sigma_1|_{max} = 425.4$ (MPa) at $\begin{array}{l} x = 4.125 \\ y = 5.875 \end{array}$ (mm)

$|\sigma_2|_{max} = -721.5$ (MPa) at $\begin{array}{l} x = 1.625 \\ y = 5.125 \end{array}$ (mm)

(b)

$|\sigma_1|_{max} = 259.6$ (MPa) at $\begin{array}{l} x = 4.125 \\ y = 3.875 \end{array}$ (mm)

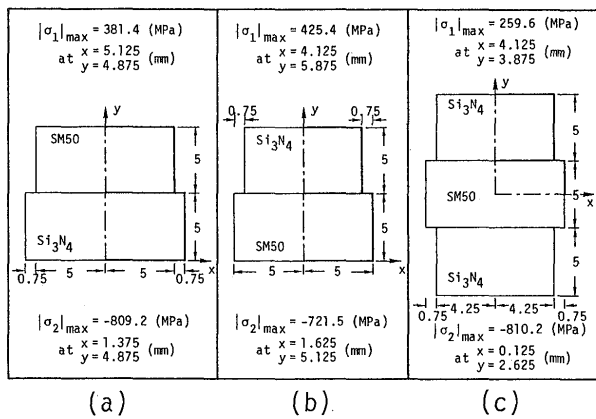$|\sigma_2|_{max} = -810.2$ (MPa) at $\begin{array}{l} x = 0.125 \\ y = 2.625 \end{array}$ (mm)

(c)

Fig.11 Effect of joint configuration (varying the dimensions of the ceramic and metal substrate) on the $|\sigma_1|_{max}$ value.

3.2.3 Relative dimensions of the ceramic and metal substrates

The size of steel substrate is the same the standard model and only the size of ceramic substrate is changed in this case.

In **Figure 11(a)** the $|\sigma_1|_{max}$ value is decreased to 78% of that in the standard model when the Si_3N_4 substrate is wider than the steel component (because the bending moment produced by the joining operation is decreased). As shown in **Figure 11(b)**, if the ceramic substrate is small compared with the steel substrate, the value of $|\sigma_1|_{max}$ is 87% of that in the standard model. Moreover, the sandwich assembly (**Figure 11(c)**) has the lowest $|\sigma_1|_{max}$ value (it is 53% of that in the standard model).

3.2.4 Consideration

A number of techniques are commonly used for evaluating the bond strength in dissimilar joints, e.g., tensile, bend and shear testing. The joint configurations illustrated in Figure 11 are generally used since the test specimens are relatively easy to produce. Bearing this in mind, the mechanical characteristics of these specimen geometries have been examined using the thermal elastic-plastic analysis described previously.

The $|\sigma_1|_{max}$ values are 78% (Figure 11(a)), 87% (Figure 11(b) and 53% (Figure 11(c)) of that produced in the standard model. In each case the $|\sigma_1|_{max}$ value is smaller than in that in actual joining situations, i.e., the laboratory test values are non-conservative. This effect must be carefully considered when ceramic/metal joint strength properties are assessed in complex fabricating situations.

4. Conclusions

Solid-state joining of silicon nitride to SM50 steel was modelled using a thermal elastic-plastic analysis. It has been confirmed that:

1. The principal stress component, σ_1, attains a maximum value, $|\sigma_1|_{max}$ ($= (\sigma_y)_{max}$), perpendicular to the bondline at the periphery of the joint in ceramic material immediately adjacent to the bondline. σ_2 is strongly compressive along the bondline. It is suggested that the maximum principal stress value ($|\sigma_1|_{max}$) perpendicular to the joint interface at the periphery of the joint, is associated with crack initiation and that the direction of crack propagation depends on the σ_2.

2. σ_x (or σ_2) is tensile in the lower mid-section of the ceramic and becomes compressive at the bondline. Because of this, a large anticlockwise bending moment is produced by the dissimilar joining operation (Figure 3).

3. There is an optimum insert layer thickness and the insert layer should have low yield stress and high ductility. However, it is important to point out that the final joint strength of dissimilar joints will not be detrimentally influenced by the yield stress of the insert layer employed.

4. Crack susceptibility can be reduced by decreasing the anticlockwise bending moment produced in the dissimilar joint. This is equivalent to decreasing the $|\sigma_1|_{max}$ value produced during the dissimilar joining operation. The joint configurations which reduce the anticlockwise bending moment produced by dissimilar joining comprise:

   a). sandwich assemblies, where the lower strength substrate is placed at the center of the sandwich,

   b). joint designs where the ceramic is made wider than the steel substrate,

   c). joint configurations (geometries) chosen so that the neutral axis of bending decreases the anticlockwise bending moment produced during dissimilar joining.

5. When the joint strength is measured, the use of specimen geometries which facilitate easy test specimen manufacture are associated with lower bending moment and $|\sigma_1|_{max}$ values. This feature must be taken into account when the laboratory strength results are applied in complex fabricating situations.

References

1) For example, A. Suzumura, T. Onzawa: Ceramic-Metal Composing and Joining Technology - Recent Aspects Technical Problem -, Journal of The Japan Society of Mechanical Engineers, 89-811(1986), 590 (in Japanese)

2) For example, Y. Ishida: Joining of New Engineering, Materials -present and Future-, Journal of The Japan Society of Mechanical Engineers, 90-821(1987), 451 (in Japanese)

3) T. Terasaki, K. Seo, T. Hirai: Dominating parameters of Residual Stress Distribution, Quarterly Journal of The

Japan Welding Society, 5-4(1987), 103 (in Japanese)

4) T. Terasaki, T. Hirai, K. Seo: Effect of Material Constant and Specimen Size on Residual Stress, Quarterly Journal of The Japan Welding Society, 6-2(1988), 89 (in Japanese)

5) T. Enjyo: Materials Evaluation and Reliability for Technique of Solid State Bonding, Summer School Note in Welding Engineering, A course, (1987),1 (in Japanese)

6) M. Miyagawa, T. Yada, K. Koguchi, T. Honzawa: Reliability Evaluation of Joints of Ceramics and Metal (I), Transaction of The Japan Society of Mechanical Engineers, 54-507(1988), 1949 (in Japanese)

7) For example, K. Suganuma et al.: Metals Science and Technology, 11-2(1986), 1156

8) For example, T. Yamada, A. Kohno: Relaxation of Termal Stress in Metal-Ceramic Bonding, Bulletin of The Japan Institute of Metal, 25-5(1986), 424 (in Japanese)

9) For example, A. Kawasaki, R. Watanabe: Finite Element Analysis of Thermal Stress of the Metal/Ceramic multi-Layer Composites with Controlled Compositional Gradients, Journal of The Japan Institute of Metals, 51-6(1987), 525 (in Japanese)